Fabricating Janus Membranes via Physicochemical Selective Chemical Vapor Deposition

Mahdi Mohammadi Ghaleni[1], Elham Tavakoli[2], Mona Bavarian[2], and Siamak Nejati[1]

[1]University of Nebraska-Lincoln
[2]Affiliation not available

April 28, 2020

Abstract

Membranes with asymmetric wettability-Janus membranes-have recently received considerable attention for a variety of critical applications. Nonetheless, the current methods for making such membranes are still challenging. Here, we report on a simple approach to introduce asymmetric wettability into hydrophilic porous domains. Our approach is based on the physicochemical-selective deposition of polytetrafluoroethylene (PTFE) on hydrophilic polymeric substrates. The physicochemical inhibition was achieved through prefilling the substrates with glycerol, containing a known amount of free radical inhibitors. We showed that the glycerol/inhibitor mixture hinders the deposition of PTFE within the membrane pores. As a result, the surface of the substrates remains open and porous. The fabricated Janus membranes show stable wetting-resistant properties, evaluated through sessile drop contact angle measurements and direct contact membrane distillation (DCMD).

Significance

Membranes with asymmetric wettability (Janus membranes) bring a new feature to the field of membrane science. Here, we developed a scalable and high-precision method for imparting asymmetric wettability to the porous substrates. The thickness and surface topography of the integrated domains are tailored based on the requirements of a specific application. The developed method is scalable and is performed in a roll-to-roll manner.

Introduction

With the recent advances in surface functionalization methods, the fabrication of porous domains with special wettability has become one of the leading research areas in the field of membrane science.[1–7] Currently, one of the primary topics in this area is the fabrication of Janus membranes -membranes with asymmetric wettability. Janus membranes bring novel functionalities, not achievable using conventional membrane processes, to membrane-based processes.[8–11] Given this asymmetric wettability, Janus membranes offer an additional means to regulate the transport of species in a designated direction.[12] This unique feature makes these membranes an attractive candidate for many applications such as ion gating,[4] oil/water separation,[3] interfacial mass transport,[13] energy harnessing,[14] anti-gravity capillary water pumps,[15] bubble aeration,[16] and water desalination.[17]

To date, extensive research exists on the fabrication of Janus membranes for different applications.[18–22] Fabrication methodologies are classified into two main categories, interfacial and non-interfacial strategies.[23] Interfacial methods typically add a new layer or interface to the substrates. As a result, additional resistance is introduced to the transport of species across the membrane. In comparison, non-interfacial strategies are not limited to the surface. The non-interfacial strategies refer to the techniques in which asymmetric wettability is formed within the porous substrate. Chemical vapor deposition and atomic layer deposition are among the promising non-interfacial strategies for altering the wettability of porous media.[23,24] However,

it is still challenging to limit the wettability modification to the surface or a specific region within the porous domains.[23,25] Therefore, despite the promising advantages of Janus membranes, the complexities involved with the fabrication schemes of these membranes have hindered their development on a large scale.

Here, we developed a simple method, based on the selective deposition of fluoropolymers onto porous media. We utilized initiated chemical vapor deposition (iCVD) to synthesize polymeric domains from the vapor phase and coated the outermost layers of various hydrophilic porous substrates. By infiltrating nonvolatile liquids containing polymerization inhibitors, we limited the deposition of the fluoropolymer to the surface and prohibited the bridging of polymer films over the pores of the substrate. We examined the performance of the fabricated Janus membranes in both static and dynamic tests.

Experimental Methods

Materials and chemicals

Hydrophilic polyvinylidene fluoride (Durapore®, 0.22 μm, 47 mm) and cellulose acetate (0.45 μm, 47 mm) membranes were purchased from Millipore Sigma. Perfluorobutane sulfonyl fluoride (PBSF, 96%) and hydroquinone (HQ) (>99%) were purchased from Sigma-Aldrich. Isopropyl alcohol (IPA, ACS grade), glycerol (certified ACS), and sodium chloride (NaCl, ACS grade) were purchased from Fisher Scientific. Ethylene Glycol (99.5%) was purchased from ACROS Organics. Hexafluoropropylene oxide (HFPO) was purchased from Oakwood chemical. Deionized (DI) water was obtained from a Simplicity® ultrapure water purification system (Millipore, Billerica, MA). Ultrapure nitrogen was purchased from Matheson Gas Company.

Initiated chemical vapor deposition (iCVD) of PTFE

The PTFE coating was deposited onto hydrophilic substrates using a custom-made iCVD reactor with a volume of 3600 cm^3. For each deposition, a hydrophilic membrane, prefilled with glycerol/inhibitor mixture (5000 ppm), was placed on the reactor stage, which was cooled to 15 °C via a recirculating chiller (Thermo Fisher Scientific). The monomer, HFPO, was metered into the reactor using a mass flowmeter (MKS Instruments) with a flow rate of 12 sccm. The PBSF jar was maintained at 27 °C to provide a constant flow rate of 1 sccm, adjusted using a precision needle valve (Swagelok). A pressure transducer (MKS Instruments) and an automated butterfly valve, connected to a vacuum process controller (MKS Instruments), were used to maintain the reactor pressure at the set point (300-1200 mTorr). For activating the initiator through thermal pyrolysis, a filament array of phosphor bronze (Goodfellow), suspended 2 cm above the substrate, was heated resistively to 350°C.

Membrane characterization

Scanning electron microscopy (SEM) images were taken using the FEI Helios NanoLab 660 microscope. To reduce the moisture content, we dried the samples in a vacuum oven set at 60 °C for three hours. After drying, the samples were cut to size, mounted on the SEM stub, and coated with 60 nm of gold, using a Ted Pella sputtering machine (108-Auto). Fourier-transform infrared spectroscopy (FTIR) measurements were performed using the attenuated total reflection (ATR) module of Bruker Alpha-p. A small (1 cm × 1 cm) sample was cut to size and placed on the diamond crystal of the ATR module. The FTIR measurements were performed using 24 high-resolution scans on each sample with a resolution of 4 cm^{-1}. The liquid contact angles on the membrane surfaces were measured using an optical tensiometer (Rame-hart, Model 590) and the sessile drop method. A 5 μL liquid droplet was placed on the dried membrane sample. We performed the measurements on three random points on each sample and presented the data with one standard deviation. The liquid entry pressure (LEP) and gas permeation measurements were performed using a custom-made porometer setup described elsewhere.[26] The overhead space of the membrane in the filter holder was filled with DI water. Subsequently, the pressure behind DI water was increased gradually. The LEP is reported as the pressure at which gas flow is detected by the flowmeter, placed inline at the outlet of the filter holder. We performed three measurements and presented the data with one standard deviation. For the gas permeation test, we flowed ultrapure nitrogen into the membrane at different pressures ranging from 2 to 40 kPa. The nitrogen permeation through the membrane was recorded using a digital flowmeter (Omega

2

Engineering, FMA1820A), connected to a computer. We characterized three membranes and presented the data with one standard deviation. The DCMD performances for the Janus membranes were evaluated using a laboratory-scale DCMD unit described elsewhere.[27] We placed the membrane into a custom-built cell with a channel dimension of 26 mm in length, 26 mm in width, and 3 mm in depth. The effective membrane area exposed to feed and distillate streams was about 6 cm^2, with the hydrophilic side facing the feed stream. The temperatures of feed and permeate streams were maintained at 70 °C and 20 °C, respectively. The water vapor flux across the membrane (J) was determined by the gravimetric method.[27]

Results and Discussion

Figure 1 illustrates the representative images of the membrane surfaces and the schematic of the procedure used to impart asymmetric wettability into hydrophilic substrates. Our fabrication scheme had three consecutive steps, shown in Figure 1 (a). In Step (i), the support was filled with glycerol/inhibitor (HQ) mixture. The detailed procedure for filling the support with liquid mixture can be found in Section S1, Supporting Information. Subsequently, in Step (ii), the filled membrane was placed on the cooled stage (15 °C) of the iCVD reactor, and the deposition of polytetrafluoroethylene (PTFE) is performed at a pressure of 900 mTorr for different times (e.g., five minutes). After the PTFE deposition, in Step (iii), the glycerol/inhibitor mixture was removed from the sample by placing the substrate in an isopropyl alcohol (IPA) bath. To visualize the glycerol/inhibitor removal, we placed the coated support on the top of an IPA/Water (50/50 v.%) bath, shown in Movie S1, Supporting Information. It can be clearly seen that the glycerol/inhibitor mixture is diffusing from the membrane into the bath. Figure 1 (b) shows a top-down scanning electron microscopy (SEM) image of the PVDF support. In that image, the top surface of the PVDF support has an open and interconnected structure. Figures 1 (c) and (d) also show the top-down and cross-section SEM images of the dried Janus membrane, respectively, fabricated through the described process. As shown, the deposited PTFE has a particulate-like structure on the top of the sponge-like structure of hydrophilic PVDF support; in the image we separated these areas using a dashed line. Moreover, the SEM images show that the top surface of membranes remained open after PTFE deposition. As a control experiment, we performed the same operation on porous PVDF supports, under the same operational conditions for iCVD, without wetting the membranes. The results indicate that the substrate, not prefilled with our liquid mixture, was blocked, and nitrogen did not flow through these substrates.
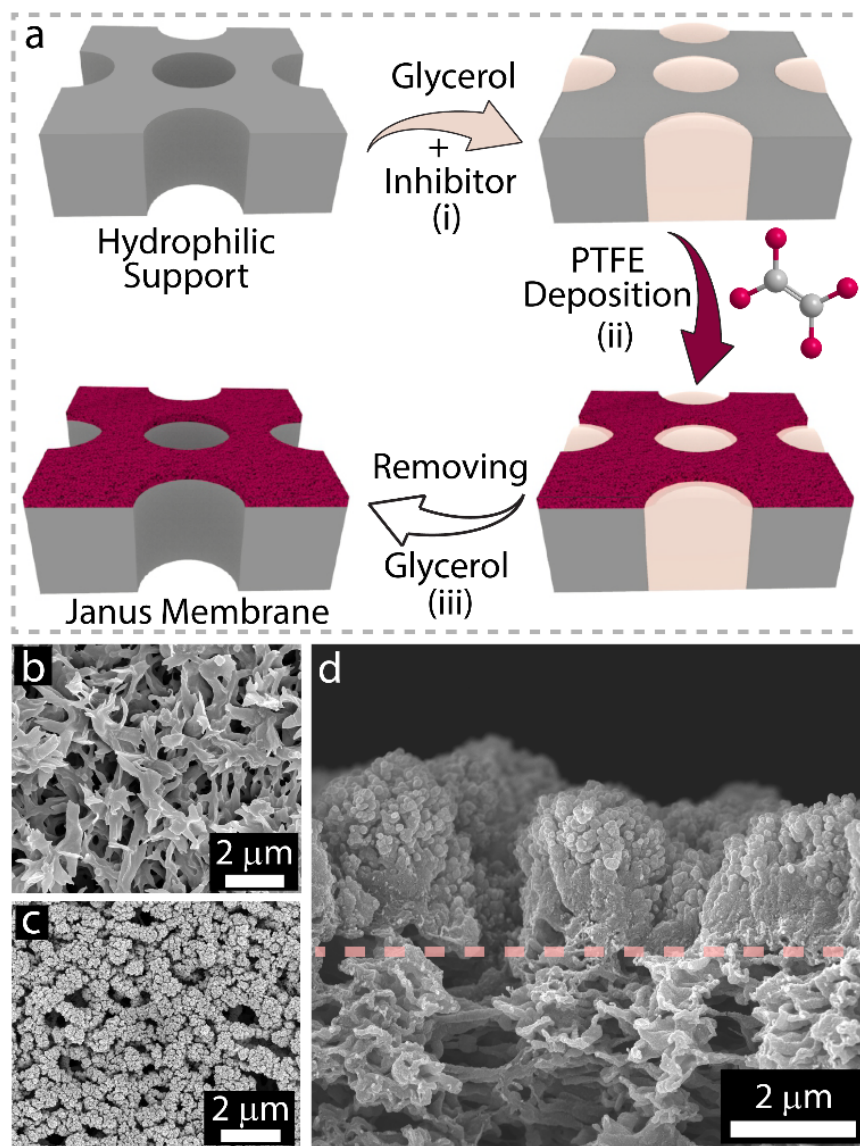
Figure 1. Fabrication of Janus membranes using physicochemical inhibition. (a) A schematic of a three-step process for the fabrication of a Janus membrane. Step (i): the hydrophilic support is filled with glycerol/inhibitor (HQ) mixture. Step (ii): the filled membrane is placed on the back-cooled stage (15 °C) of the iCVD reactor, and the PTFE deposition is performed for a specific time (5-15 min). Step (iii): the glycerol/inhibitor mixture is removed from the sample by placing it inside an isopropanol bath. (b) A top-down representative scanning electron microscopy (SEM) image of the hydrophilic PVDF support. (c) A top-down SEM image of the Janus membrane surface showing the PTFE structure deposited on the top surface of the support without blocking the pores. (d) A cross-section SEM image of the Janus membrane surface showing the PTFE structure deposited on the hydrophilic PVDF support. The dashed line shows the PVDF-PTFE interface. Here, the pressure and time of deposition were 900 mTorr and five minutes, respectively.

Although it has been shown that, [28–30] by changing the iCVD condition and moving from a diffusion-limited process toward a reaction-limited process, we are able to apply polymeric coating within the entire porous

4

substrates, selective area deposition of polymers has not yet been achieved. Here, using the developed approach, we show that the PTFE deposition can be limited to the solid domains on the top surface of the substrate. As a result, the surface porosity of the substrate does not decrease after the coating. In the developed method, we note two different inhibition mechanisms: physical and chemical. Once the primary radicals are absorbed into the glycerol mixture, the relatively faster rate of diffusion, compared to that of the surface diffusion, prevents the formation of a polymer film on the liquid surface. As a result, the deposition of PTFE on the liquid domain will be delayed. The proposed mechanism can be found in Section S2, Supporting Information. In addition to the physical inhibition, the chemical inhibition also exists because of the quenching of the absorbed radicals in glycerol through the HQ present in the liquid mixture.

To unravel the difference between physical and chemical inhibition, we performed similar experiments on liquid films. For this purpose, the liquid films were prepared via spin-coating of the glycerol/inhibitor mixture on pieces of the silicon wafer with comparable areas. The detailed information for sample preparation can be found in Section S3, Supporting Information. Figure 2 (a) shows the Fourier transformed infrared spectroscopy (FTIR) of liquid samples before and after five minutes of PTFE deposition. As shown, the FTIR spectra of glycerol/inhibitor mixture remained unchanged after five minutes of iCVD deposition, indicating that no detectable PTFE was deposited on the surface of the glycerol/inhibitor. On the other hand, the PTFE characteristic peaks, located between 1150-1225 cm^{-1}, were salient in the spectra of the pure glycerol sample processed in the iCVD chamber. This observation indicates that, during the first five minutes of reaction, HQ molecules present in glycerol quenched the adsorbed primary radicals. Increasing the deposition time to seven minutes, we found that the inhibition process becomes ineffective, and the characteristic peaks of PTFE were again observed in the spectra. The data showing the FTIR of the samples processed for a longer time are shown in Section S3, Supporting Information.
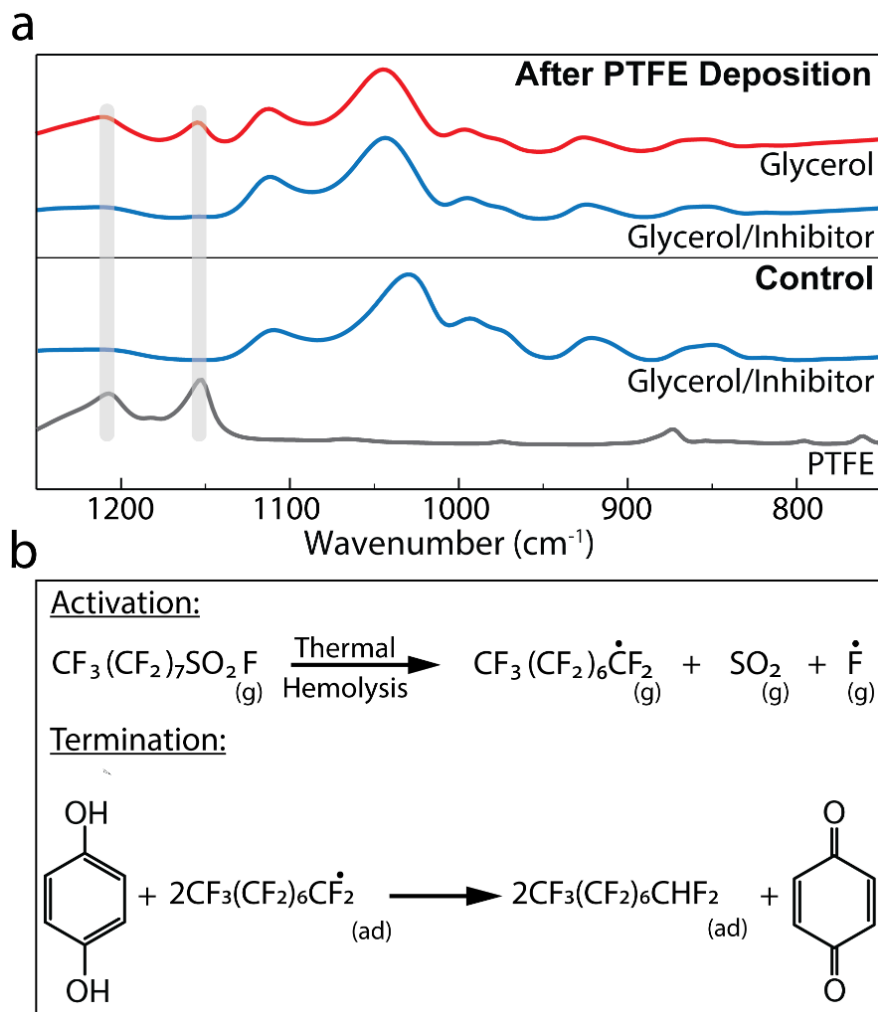
Figure 2. (a) Comparison of FTIR spectra of glycerol and glycerol/inhibitor mixture before (control) and after 5 min PTFE deposition. Here, to make the substrate, an equal amount (30 µl) of corresponding solution was spin-coated on plasma-cleaned Si substrates, with comparable areas. Then, PTFE deposition was performed in the iCVD reactor within 5 min at T_S=15 °C and P=300-1200 mTorr. (b) The reaction pathway for thermal hemolysis activation of the initiator in the gas phase followed by quenching the primary free radicals on the liquid surface.

As mentioned earlier, for the samples prewetted by the glycerol/HQ, both chemical and physical mechanisms are in action. The deposition was limited to the top surfaces and the liquid prevents the reactants from coating the inner walls of the porous support. At the same time, HQ quenches the free radicals absorbed into glycerol. Figure 2 (b) shows the pathway for thermal hemolysis (activation) of the initiator (perfluorobutane sulfonyl fluoride),[31] and the proposed reaction for chemical inhibition. We propose that the primary radicals (), adsorbed on the surface of glycerol/inhibitor mixture, are quenched by HQ, through electron transfer.[32,33] The FTIR results of the glycerol/inhibitor mixture after primary radical adsorption also showed that HQ is reduced to quinone, confirming that HQ inhibits polymerization by quenching the radicals; see Section S3, Supporting Information.

To investigate the effectiveness of physicochemical inhibition, we evaluated the surface porosity of PVDF support by measuring nitrogen permeation at various transmembrane differential pressures. The PTFE

deposition was performed at different pressures ranging from 300 to 1200 mTorr. Figure 3 (a) compares the nitrogen permeation for the pristine PVDF support with those of coated samples prepared at different iCVD pressures. As shown, we did not observe any significant reduction in nitrogen permeation after depositing of PTFE. This observation indicates the deposition was limited to the solid domains, and the surface porosity of the membranes was preserved.

To measure the wettability of the substrates, we performed the water contact angle (CA) measurement on the top and bottom surface of the processed membranes. Figure 3 (b) shows that the water CA on the top surface of all samples was above 140 degrees. In contrast, the water droplet placed on the back side of the membrane wicks through. We note that the contact angle of water on the top surface of the Janus membranes increases with increasing the pressure of iCVD processing. Section S4, Supporting Information, includes the SEM images showing the effect of varying the deposition pressure on the morphology of Janus membrane surfaces. Here we attribute the observed trend in the membranes' CA to the induced roughness as a result of a transitionig the deposition process from the adsorption limited to a gas-phase limited one [34] Figure 3 (c) also shows the optical image of water and ethylene glycol droplets placed on the top and the back side of the Janus membranes. As shown, both liquids formed contact angles above 140 degrees on the top surface of the Janus membrane. However, the contact angle of all liquids on the back side was zero. This observation shows that the back side of the membrane remained pristine. The X-ray photoelectron spectroscopy (XPS) C1s core electron spectra collected from the bottom surface of the coated membrane also matched that of a pristine PVDF; see Section S5, Supporting Information.

To examine the underwater oleophobic properties of the hydrophilic side of the Janus membranes, we measured the contact angle for oil droplets when the hydrophilic side is immersed in water. Figure 3 (d) displays the side-view optical image from a fabricated Janus membrane placed on the water surface with the hydrophilic side facing the water. As shown, the oil droplet has a contact angle of ~140 degrees with the membrane and does not wet the surface, confirming underwater oleophobicity of the untreated side. To illustrate this functionality more clearly, we recorded a video of the testing procedure of a Janus membrane, shown in Movie S2, Supporting Information. As shown, after suspending a Janus membrane on the top surface of a water bath, water penetrates the Janus membrane such that the membrane becomes semi-transparent. However, the thin PTFE layer (2-3 µm) hinders water from reaching the top surface. As a result, when water droplets impinged on the top surface of the Janus membrane, they bounced back off the surface due to the air gap formed within the PTFE domain; see Movie S2, Supporting Information.
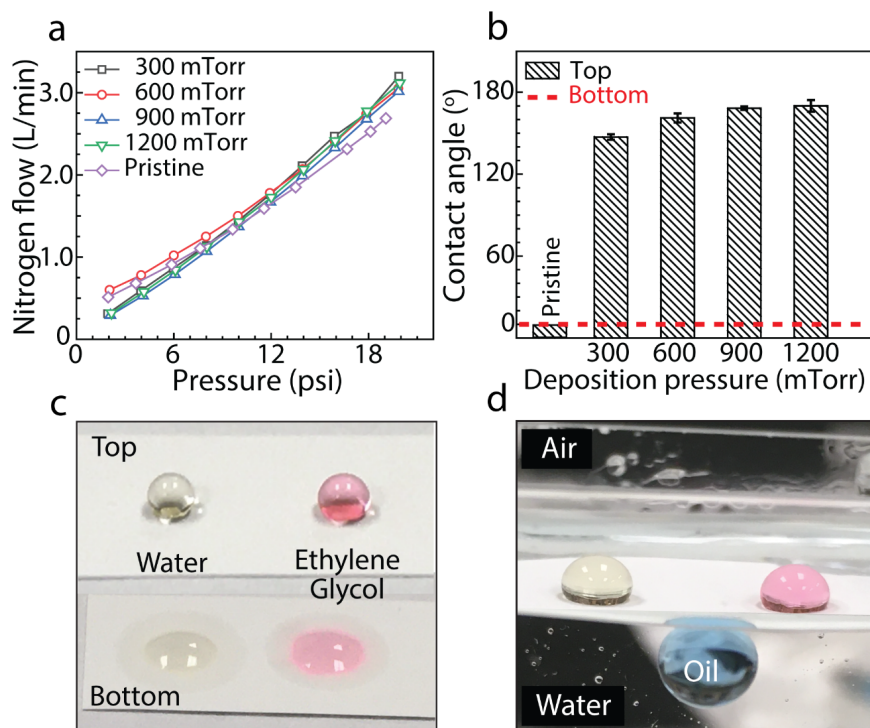
Figure 3. The characterization results of the Janus membrane fabricated by selective infiltration of PTFE on the hydrophilic PVDF supports. (a) Comparison of nitrogen flow rate into the pristine PVDF with those of Janus membranes made at different deposition pressures (300-1200 mTorr). (b) Water contact angle on the top (coated) and the bottom surface of Janus membranes fabricated at different deposition pressures (300-1200 mTorr). Here, the water contact angle on the bottom (uncoated) surface of hydrophilic supports is zero. (c) The contact angle of water and ethylene glycol droplets on the top and bottom surface of the Janus membranes. Here, to make the Janus membrane, the PTFE deposition was performed at 1200 mTorr for five minutes. (b) Water and ethylene glycol droplets on a Janus membrane floating on water while oil droplet is in contact with the hydrophilic (bottom) surface immersed in water. Here, to make the Janus membrane, the PTFE deposition was performed at 900 mTorr for five minutes. To investigate the effectiveness of the deposited PTFE layer in maintaining an air gap between two liquid streams, we examined our fabricated Janus membranes in direct contact membrane distillation (DCMD) and desalinate a synthetic water solution containing 35 g/L NaCl.[17,35] Figure 4 shows the DCMD performance of the Janus membrane for 60 minutes. As shown, the salt rejection and water flux remained stable during this experiment. This observation confirms the effectiveness of fabricated schemes in the development of Janus membranes. The measured liquid entry pressure (LEP), presented in Section S6 of Supporting Information, further confirms that the fabricated Janus membranes have high wetting resistance. Using our developed approach, we further fabricated Janus membranes on a few hydrophilic substrates such as cellulose acetate and carbon nanotube-polyvinyl alcohol (CNT-PVA) composite. The images of Janus CNT-PVA composite and DCMD performance of the Janus cellulose acetate membrane are shown in Section S7, Supporting Information. Movie S3, Supporting Information, also shows the impact of water droplets on the top surface of Janus CNT-PVA composite.
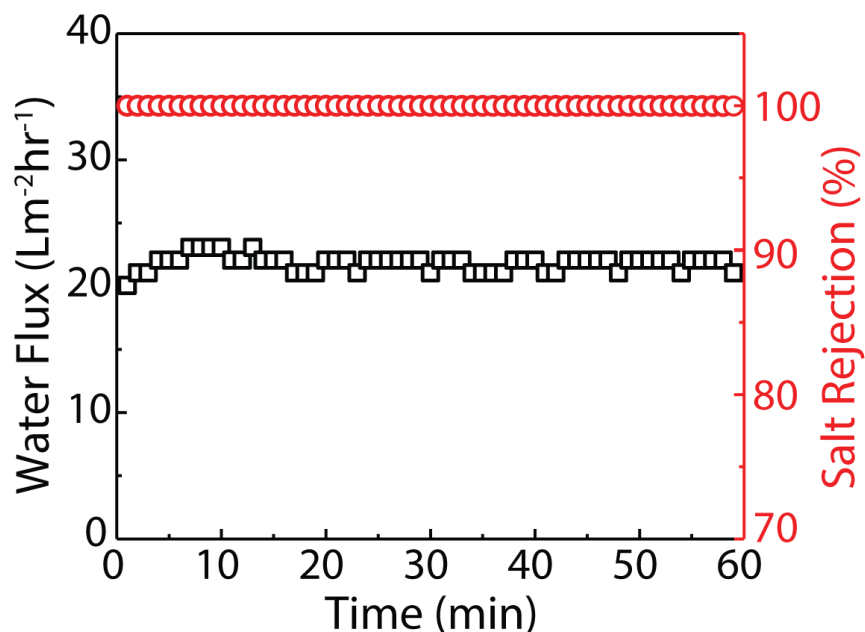
8

Figure 4. The DCMD results of Janus membranes fabricated using hydrophilic PVDF support; the pressure and time of deposition were 1200 mTorr and 15 minutes. The feed solution included 35 g/L sodium chloride. The reported porosity, thickness, and pore size of pristine PVDF supports were 70%, 125 μm, and 220 nm, respectively. The feed and distillate temperatures were kept at 70 and 20 °C, respectively. The feed and distillate flowrates also were 0.2 and 0.15 L/min, respectively.

Conclusion

We developed a scalable method for the fabrication of Janus membranes through initiated chemical vapor deposition (iCVD) of fluoropolymers on porous media. We showed that the asymmetric wettability in the hydrophilic porous substrates is created by limiting the PTFE deposition to the surface of the porous domain. This objective was achieved by filling the substrates with non-volatile liquid (glycerol) mixtures. Also, we found that the presence of a free radical inhibitor in the liquid mixtures delays the deposition of PTFE on the surface of the mixture. The characterization of the developed membranes using sessile drop contact angle measurements and membrane distillation proved the effectiveness of our approach in fabricating Janus membranes.

Acknowledgments

References

1. Zhou S, Liu F, Wang J, et al. Janus Membrane with Unparalleled Forward Osmosis Performance. *Environ Sci Technol Lett* . 2019;6(2):79-85. doi:10.1021/acs.estlett.8b00630

2. Hu J, Zhou S, Sun Y, Fang X, Wu L. Fabrication, properties and applications of Janus particles. *Chem Soc Rev* . 2012;41(11):4356. doi:10.1039/c2cs35032g

9

3. Wang Z, Wang Y, Liu G. Rapid and Efficient Separation of Oil from Oil-in-Water Emulsions Using a Janus Cotton Fabric. *Angew Chemie - Int Ed* . 2016;55(4):1291-1294. doi:10.1002/anie.201507451

4. Zhang Z, Kong XY, Xiao K, et al. A Bioinspired Multifunctional Heterogeneous Membrane with Ultrahigh Ionic Rectification and Highly Efficient Selective Ionic Gating. *Adv Mater* . 2016;28(1):144-150. doi:10.1002/adma.201503668

5. Tian X, Jin H, Sainio J, Ras RHA, Ikkala O. Droplet and Fluid Gating by Biomimetic Janus Membranes. *Adv Funct Mater* . 2014;24(38):6023-6028. doi:10.1002/adfm.201400714

6. Yang X, Wang Z, Shao L. Construction of oil-unidirectional membrane for integrated oil collection with lossless transportation and oil-in-water emulsion purification. *J Memb Sci* . 2018;549:67-74. doi:10.1016/J.MEMSCI.2017.11.0

7. Ren F, Li G, Zhang Z, et al. A single-layer Janus membrane with dual gradient conical micropore arrays for self-driving fog collection +. 2017. doi:10.1039/c7ta04392a

8. Yang HC, Hou J, Chen V, Xu ZK. Janus Membranes: Exploring Duality for Advanced Separation. *Angew Chemie - Int Ed* . 2016;55(43):13398-13407. doi:10.1002/anie.201601589

9. Li H, Yang J, Xu Z. Asymmetric Surface Engineering for Janus Membranes. *Adv Mater Interfaces* . February 2020:1902064. doi:10.1002/admi.201902064

10. Li M, Lu KJ, Wang L, Zhang X, Chung T-S. Janus membranes with asymmetric wettability via a layer-by-layer coating strategy for robust membrane distillation. *J Memb Sci* . 2020;603:118031. doi:10.1016/J.MEMSCI.2020.118031

11. Li C, Li X, Du X, Tong T, Cath TY, Lee J. Antiwetting and Antifouling Janus Membrane for Desalination of Saline Oily Wastewater by Membrane Distillation. *ACS Appl Mater Interfaces* . 2019;11(20):18456-18465. doi:10.1021/acsami.9b04212

12. Zhao Y, Wang H, Zhou H, Lin T. Directional Fluid Transport in Thin Porous Materials and its Functional Applications. *Small* . 2017;13(4):1601070. doi:10.1002/smll.201601070

13. Hou J, Ji C, Dong G, Xiao B, Ye Y, Chen V. Biocatalytic Janus membranes for CO2 removal utilizing carbonic anhydrase. *J Mater Chem A* . 2015;3(33):17032-17041. doi:10.1039/c5ta01756d

14. Zhang Z, Kong XY, Xiao K, et al. Engineered Asymmetric Heterogeneous Membrane: A Concentration-Gradient-Driven Energy Harvesting Device.*J Am Chem Soc* . 2015;137(46):14765-14772. doi:10.1021/jacs.5b09918

15. Cao M, Li K, Dong Z, et al. Superhydrophobic "pump": Continuous and Spontaneous Antigravity Water Delivery. *Adv Funct Mater* . 2015;25(26):4114-4119. doi:10.1002/adfm.201501320

16. Yang H-C, Hou J, Wan L-S, Chen V, Xu Z-K. Janus Membranes with Asymmetric Wettability for Fine Bubble Aeration. *Adv Mater Interfaces* . 2016;3(9):1500774. doi:10.1002/admi.201500774

17. Mohammadi Ghaleni M, Al Balushi A, Kaviani S, Tavakoli E, Bavarian M, Nejati S. Fabrication of Janus Membranes for Desalination of Oil-Contaminated Saline Water. *ACS Appl Mater Interfaces* . 2018;10(51):44871-44879. doi:10.1021/acsami.8b16621

18. Zhang C, Ou Y, Lei W-X, Wan L-S, Ji J, Xu Z-K. CuSO$_4$ /H $_2$ O $_2$ -Induced Rapid Deposition of Polydopamine Coatings with High Uniformity and Enhanced Stability. *Angew Chemie* . 2016;128(9):3106-3109. doi:10.1002/ange.201510724

19. Gao S, Zhu Y, Wang J, Zhang F, Li J, Jin J. Layer-by-Layer Construction of Cu $^{2+}$ /Alginate Multilayer Modified Ultrafiltration Membrane with Bioinspired Superwetting Property for High-Efficient Crude-Oil-in-Water Emulsion Separation. *Adv Funct Mater* . 2018;28(49):1801944. doi:10.1002/adfm.201801944

20. Yang H-C, Waldman RZ, Wu M-B, et al. Dopamine: Just the Right Medicine for Membranes. *Adv Funct Mater* . 2018;28(8):1705327. doi:10.1002/adfm.201705327

21. Li H, Cao M, Ma X, et al. "Plug-and-Go"-Type Liquid Diode: Integrated Mesh with Janus Superwetting Properties. *Adv Mater Interfaces* . 2016;3(19):1600276. doi:10.1002/admi.201600276

22. Wang Z, Yang X, Cheng Z, Liu Y, Shao L, Jiang L. Simply realizing "water diode" Janus membranes for multifunctional smart applications.*Mater Horizons* . 2017;4(4):701-708. doi:10.1039/C7MH00216E

23. Yang HC, Xie Y, Hou J, Cheetham AK, Chen V, Darling SB. Janus Membranes: Creating Asymmetry for Energy Efficiency. *Adv Mater* . 2018;30(43):1801495. doi:10.1002/adma.201801495

24. McGaughey AL, Karandikar P, Gupta M, Childress AE. Hydrophobicity versus Pore Size: Polymer Coatings to Improve Membrane Wetting Resistance for Membrane Distillation. *ACS Appl Polym Mater* . 2020;2(3):1256-1267. doi:10.1021/acsapm.9b01133

25. Zhou H, Guo Z. Superwetting Janus membranes: focusing on unidirectional transport behaviors and multiple applications. *J Mater Chem A* . 2019;7(21):12921-12950. doi:10.1039/C9TA02682G

26. Al Balushi A. Fabrication of Polyvinylidene Fluoride Hollow Fiber Membranes for Membrane Distillation. *MS Thesis* . August 2019. https://digitalcommons.unl.edu/embargotheses/164. Accessed March 29, 2020.

27. Nejati S, Boo C, Osuji CO, Elimelech M. Engineering flat sheet microporous PVDF films for membrane distillation. *J Memb Sci* . 2015;492:355-363. doi:10.1016/J.MEMSCI.2015.05.033

28. Nejati S, Lau KKS. Pore filling of nanostructured electrodes in dye sensitized solar cells by initiated chemical vapor deposition.*Nano Lett* . 2011;11(2):419-423. doi:10.1021/nl103020w

29. Nejati S, Minford TE, Smolin YY, Lau KKS. Enhanced Charge Storage of Ultrathin Polythiophene Films within Porous Nanostructures. *ACS Nano* . 2014;8(6):5413-5422. doi:10.1021/nn500007c

30. Lau KKS, Gleason KK. Initiated Chemical Vapor Deposition (iCVD) of Poly(alkyl acrylates): An Experimental Study. *Macromolecules* . 2006;39(10):3688-3694. doi:10.1021/ma0601619

31. Lewis HGP, Jeffrey A. Caulfield A, Gleason KK. Perfluorooctane Sulfonyl Fluoride as an Initiator in Hot-Filament Chemical Vapor Deposition of Fluorocarbon Thin Films. *Langmuir* . 2001;17:7652-7655. doi:10.1021/LA0104929

32. Valgimigli L, Amorati R, Fumo MG, et al. The Unusual Reaction of Semiquinone Radicals with Molecular Oxygen. *J Org Chem* . 2008;73:1830-1841. doi:10.1021/JO7024543

33. Guin PS, Das S, Mandal PC. Electrochemical Reduction of Quinones in Different Media: A Review. *Int J Electrochem* . 2011;2011:1-22. doi:10.4061/2011/816202

34. Mohammadi Ghaleni M, Kaviani S, Rajwade K, Bavarian M, Perreault F, Nejati S. All Dry Bottom-Up Assembly of Omniphobic Interfaces. *Adv Mater Interfaces* . 2020.

35. Mohammadi Ghaleni M, Bavarian M, Nejati S. Model-guided design of high-performance membrane distillation modules for water desalination.*J Memb Sci* . 2018;563. doi:10.1016/j.memsci.2018.06.054